Ckap2 Regulates Aneuploidy, Cell Cycling, and Cell Death in a p53-Dependent Manner

Katsuya Tsuchihara,[1] Valentina Lapin,[1] Christopher Bakal,[2,3] Hitoshi Okada,[1] Lauren Brown,[2,3] Masami Hirota-Tsuchihara,[2] Kathrin Zaugg,[1,3] Alexandra Ho,[1] Annick Itie-YouTen,[1] Marees Harris-Brandts,[2] Robert Rottapel,[2,3] Christopher D. Richardson,[2,3] Samuel Benchimol,[2,3] and Tak Wah Mak[1,2,3,4]

[1]The Campbell Family Institute for Breast Cancer Research, [2]Ontario Cancer Institute, and Departments of [3]Medical Biophysics and [4]Immunology, University of Toronto, Toronto, Ontario, Canada

Abstract

We used DNA microarray screening to identify *Ckap2* (*cytoskeleton associated protein 2*) as a novel p53 target gene in a mouse erythroleukemia cell line. DNA damage induces human and mouse *CKAP2* expression in a p53-dependent manner and p53 activates the *Ckap2* promoter. Overexpressed Ckap2 colocalizes with and stabilizes microtubules. In p53-null cells, overexpression of Ckap2 induces tetraploidy with aberrant centrosome numbers, suggesting disturbed mitosis and cytokinesis. In p53-competent cells, Ckap2 does not induce tetraploidy but activates p53-mediated cell cycle arrest and apoptosis. Our data suggest the existence of a functional positive feedback loop in which Ckap2 activates the G_1 tetraploidy checkpoint and prevents aneuploidy. (Cancer Res 2005; 65(15): 6685-91)

Introduction

Inactivation of the tumor suppressor p53 is commonly associated with tumorigenesis. p53 prevents the proliferation of aberrant cells by regulating the cell cycle and apoptosis. Once activated by DNA damage, p53 translocates into the nucleus and induces the transcription of target genes harboring p53-binding sites. Tumor-derived mutant p53 proteins lack transactivation ability, confirming the importance of p53 target genes in tumor prevention (1). Whereas many p53 target genes are known, transcriptomic and bioinformatic studies suggest that p53 induces additional genes important for tumor suppression (2, 3).

Aneuploidy is linked to genetic instability and malignant tumor progression. A frequent precursor of aneuploidy is tetraploidy, which arises from mitotic errors induced by cytoskeletal perturbation or excess mitotic kinases. Although the mechanism is not fully elucidated, p53 is frequently activated in tetraploid cells and prevents the proliferation of these cells by inducing their G_1 arrest or apoptosis (4–6).

Through DNA microarray screening of a mouse erythroleukemia cell line in which the *p53* gene carries a temperature-sensitive mutation, we identified *Ckap2* (*cytoskeleton-associated protein 2;* ref. 7) as a novel p53 target gene. Tumor-specific overexpression of human homologue of *Ckap2* has been reported in B-cell lymphoma and gastric cancer. However, biological function of this gene product has not been identified (7–9). In this study, we showed that Ckap2 protein associates with and stabilizes microtubules, and Ckap2 overexpression induces tetraploidy in the absence of p53. In p53-competent cells, Ckap2 enhances wild-type (WT) p53 activity and triggers G_1 arrest and apoptosis in a p53-dependent manner.

Materials and Methods

cDNA microarray. The mouse erythroleukemia cell line DP16.1 and its derivative DP16.1/p53ts (which bears a temperature-sensitive mutation of p53 that inactivates it at 37°C) were cultured in α-MEM supplemented with 10% FCS for 6 hours at 37°C or 32°C. Total RNA was extracted using the RNeasy total RNA extraction kit (Qiagen, Valencia, CA). Synthesis of cDNA probes using Cy3 and Cy5, hybridization of these probes to the mouse GEM1 cDNA microarray, and signal intensity analyses were done by IncyteGenomics, Inc. (Palo Alto, CA).

Prediction of promoter and p53-binding sites. Mouse and human genomic DNA sequences were obtained from National Center for Biotechnology Information Entrez Gene (http://www.ncbi.nlm.nih.gov/entrez/query.fcgi?db=gene). Promoter sequences were predicted using WWW Promoter Scan program (http://www-bimas.cit.nih.gov/molbio/proscan/; ref. 10). Potential p53-binding sites were sought using TFBIND (http://tfbind.hgc.jp/; ref. 11).

Cell culture and DNA transfection. E14K embryonic stem cells (129/Ola) were maintained on 1% gelatin-coated dishes in DMEM supplemented with leukemia inhibitory factor, 15% FCS, L-glutamine, and β-mercaptoethanol. NIH3T3 cells and MCF-7 cells were maintained in DMEM supplemented with 10% FCS. The human cell lines HCT116 and HCT116 $p53^{-/-}$ were generously provided by Dr. B. Vogelstein (Sidney Kimmel Comprehensive Cancer Center, Baltimore, MD) and maintained in McCOY5A medium supplemented with 10% FCS and L-glutamine. Transient transfections were done using LipofectAMINE 2000 (Invitrogen, Carlsbad, CA).

Northern blotting. Total RNA was isolated using the RNeasy total RNA extraction kit (Qiagen) and samples (10 μg) were fractionated, probed, and visualized using standard protocols.

Western blotting. Total cell lysates (10-20 μg) were prepared, fractionated, and blotted according to standard protocols. Anti-Ckap2 antiserum was raised in rabbits against a purified 6× histidine-tagged Ckap2 fusion protein and affinity-purified on GST-Ckap2 Sepharose beads. Other antibodies were as follows: rabbit anti-mouse p53 (CM5; Novocastra, Newcastle upon Tyne, United Kingdom); mouse anti-human p53 (Ab-6), anti-mouse $p21^{Waf1}$ (Ab-4), anti-human $p21^{WAF1}$ (Ab-3; all from Calbiochem, Darmstadt, Germany); and rabbit anti-actin (Sigma, St. Louis, MO).

Mammalian expression vectors. Mouse expressed sequence tags (EST) clone BF168983 contained the full-length *Ckap2* cDNA sequence. Human EST clone BU178846 contained the full-length *CKAP2* cDNA sequence. These EST clones has been subcloned into the pCMV-SPORT6

Note: Supplementary data for this article are available at Cancer Research Online (http://cancerres.aacrjournals.org/).

K. Tsuchihara is currently at National Cancer Center Research Institute East, Kashiwa, Chiba, Japan.

Requests for reprints: Tak W. Mak, The Campbell Family Institute for Breast Cancer Research, 620 University Avenue, Suite 706, Toronto, Ontario, Canada M5G 2C1. Phone: 416-946-2234; Fax: 416-204-5300; E-mail: tmak@uhnres.utoronto.ca.

vector (Invitrogen) and used for mouse Ckap2 (pSPORT6-Ckap2) or human CKAP2 (pSPORT6-CKAP2) expression in mammalian cells. For expression of full-length Ckap2 bearing a COOH-terminal enhanced green fluorescent protein (EGFP) tag, a full-length *Ckap2* cDNA fragment without a stop codon was amplified by PCR from BF168983 and subcloned into the EGFP expression vector pQBI25 (Qbiogene, Carlsbad, CA) to generate pQBI25su-Ckap2 (1-648). A series of deletion mutant cDNAs were amplified by PCR using pQBI25-Ckap2 (1-648) as a template, and subcloned into pQBI25.

Luciferase assays. DNA fragments derived from the upstream region of the *Ckap2* and *CKAP2* genes were amplified by PCR from the 129/SvEvTAc mouse phage artificial chromosome clone 638C11 (BACPAC Resources Center, Children's Hospital Oakland Research Institute, Oakland, CA), and genomic DNA of HCT116 cells, respectively. Amplified DNA fragments were subcloned into either the pGL3-Basic or pGL3-Promoter vectors (Promega, Madison, WI) to generate pro-Luc constructs as detailed in Supplementary Methods. These constructs were cotransfected into HCT116 $p53^{-/-}$ cells with either empty pcDNA3 vector or pcDNA3 vector expressing p53. Luciferase activity was measured and normalized as described in Supplementary Methods.

Chromatin immunoprecipitation. Chromatin immunoprecipitation (ChIP) assays were done using the Acetyl-Histone H3 ChIP Assay Kit (Upstate Biotechnology, Charlottesville, VA). Anti-mouse p53 (CM5) was used for immunoprecipitation. PCR amplifications of the promoter regions of the *Ckap2* gene containing the consensus p53-binding sequences (−359 to −159 and −409 to −186), and of intron 1 that lacks a p53-binding site (+238 to +405), were done on immunoprecipitated chromatin using specific primers and conditions as detailed in Supplementary Methods.

Immunofluorescence microscopy. HCT116, HCT116 $p53^{-/-}$, and NIH3T3 cells were transfected with pQBI-Ckap2 (1-648) and its variants. At 48 hours posttransfection, cells were preextracted and fixed as previously described (12). The following primary and secondary antibodies were used: mouse anti-bovine tubulin (Invitrogen) mouse monoclonal anti–acetyl-tubulin (6-11B-1, Sigma), mouse monoclonal anti–γ-tubulin (GTU-88, Sigma), and Alexa Fluor 594 goat anti-mouse IgG (Molecular Probes). Images were obtained using an Olympus 1X-70 inverted microscope and Deltavision Deconvolution Microscopy software (Applied Precision, Issaquah, WA).

Reverse transcription-PCR. Mouse *Ckap2*, $p21^{Waf1}$, and *actin* in DP16.1 and mouse embryonic stem cells were detected by reverse transcription-PCR (RT-PCR). Primers and conditions are detailed in Supplementary Methods. HCT116 cells were transfected with pQBI25-Ckap2 (1-648), pQBI25-Ckap2 (1-382), or pQBI25 along with 0.2 μg of a vector expressing the puromycin resistance gene (pBabe-puro; ref. 13). Transfected cells were selected by 48 hours culture in 10 μg/mL puromycin. Total RNA was purified from 1×10^4 cells using Superscript III CellsDirect cDNA Synthesis Kit (Invitrogen). Synthesized cDNA (1%) was subjected to RT-PCR using previously described primer sets and PCR conditions (14).

5-Bromo-2′-deoxyuridine incorporation. 5-Bromo-2′-deoxyuridine (BrdUrd) incorporation was done using the BrdUrd Labeling and Detection Kit I (Roche, Basel, Switzerland) with some modifications. HCT116 and HCT116 $p53^{-/-}$ cells were plated on glass slides and transfected with pQBI25-Ckap2 (1-648), pQBI25-Ckap2 (1-382), or pQBI25. Transfected cells were labeled with BrdUrd 48 hours after transfection. Cells were fixed with 2% paraformaldehyde and permeabilized with 0.1% Triton X-100. Incorporated BrdUrd was visualized using anti-BrdUrd and Alexa Fluor 594 anti-mouse IgG. At least 100 cells were examined per transfection.

Cell death and apoptosis assay. For apoptosis, TUNEL assays were done using the In Situ Cell Death Detection Kit (Roche). For cell death, HCT116 cells (5×10^5) were plated in six-well plates and transfected with 0.8 μg Ckap2 expression vectors and 0.2 μg EGFP expression vector. Transfected cells were observed by fluorescence microscope 48 hours after transfection. Cellular morphology was examined and percentages of GFP-positive cells with aberrant versus normal morphology were calculated.

Results

***Ckap2* is a p53 target gene.** The mutant p53 adopts a WT conformation at 32°C and induces transcription of downstream genes in DP16.1/p53ts cells (15). The transcriptomes of DP16.1/p53ts cells cultured at 37°C versus 32°C were screened with the mouse EST microarray chip. Using a cutoff ratio of 2.3 and a fold up-regulation minimum of 2.4, we isolated 32 ESTs induced by p53. Northern blotting showed that 10 were independent novel p53 targets (data not shown), including EST W11380, which represented a partial murine *Ckap2* cDNA (7).

To confirm that p53 induced Ckap2, we examined mRNA and protein expression in DP16.1/p53ts cells using full-length *Ckap2* cDNA for Northern blotting, RT-PCR, and rabbit antiserum against full-length recombinant Ckap2 protein for Western blotting. Both mRNA and protein levels of Ckap2 were increased in DP16.1/p53ts cells (but not the parental $p53^{-/-}$ DP16.1 cells) shifted from 37°C to 32°C (Fig. 1*A*). We then treated WT mouse embryonic stem cells with various DNA-damaging agents. *Ckap2* mRNA and protein were induced by γ-irradiation and etoposide treatment, but not by UV irradiation (Fig. 1*B*). The control p53 target gene $p21^{WAF1}$ was induced by all stimuli tested.

Human *CKAP2* undergoes alternative splicing that generates two major transcripts and proteins in multiple tissues and cell lines (8). We used our rabbit anti-Ckap2 antiserum (which cross-reacts with both human CKAP2 proteins) to investigate whether human CKAP2 proteins are also up-regulated by p53. The human colon cancer cell line HCT116, and its derivative HCT116 $p53^{-/-}$ (in which both p53 alleles are deleted), were treated with γ- or UV irradiation. Both CKAP2 proteins were induced in HCT116 but not in HCT116 $p53^{-/-}$ cells (Fig. 1*C*). γ-irradiation of the human cell line MCF-7, which expresses WT p53, also resulted in CKAP2 induction (Fig. 1*C*).

p53 transactivates the *Ckap2* promoter. To determine whether p53 up-regulates Ckap2 via transactivation, we cloned a genomic DNA fragment containing the mouse *Ckap2* gene from a mouse phage artificial chromosome library. The upstream region of the *Ckap2* gene was analyzed with a promoter prediction program. A site 300 bp upstream of *Ckap2* exon 1 appeared to contain a TATA-less promoter (Fig. 1*D*) with a highly conserved p53-binding site. This site matched the consensus p53-binding site (16) at 18 of 20 bp with no spacer between the two half sites. In the human *CKAP2* locus, a putative p53-binding site was found 7 kb upstream of *CKAP2* exon 1 (Fig. 1*D*).

We used ChIP assays to investigate whether p53 protein could bind to the predicted p53-binding site in the *Ckap2* promoter. Lysates of DP16.1/p53ts cells grown at 32°C for 8 hours were immunoprecipitated using anti-p53 antibody followed by PCR amplification. Only the region of *Ckap2* promoter containing the p53-binding site was specifically amplified from the genomic DNA fragment coimmunoprecipitated with p53 protein (Fig. 1*E*).

To determine whether p53 could induce *Ckap2* promoter activity, a series of DNA fragments upstream of *Ckap2* were subcloned into a luciferase reporter gene expression vector (free of enhancers or promoters) and transfected into HCT116 $p53^{-/-}$ cells that also received, or did not receive, a plasmid conferring p53 expression. Reporter constructs containing the putative *Ckap2* promoter (−440 Ckap2-pro-Luc, −294 Ckap2-pro-Luc, −265 Ckap2-pro-Luc) showed detectable luciferase activity in $p53^{-/-}$ cells, suggesting that the basal activity of the *Ckap2*

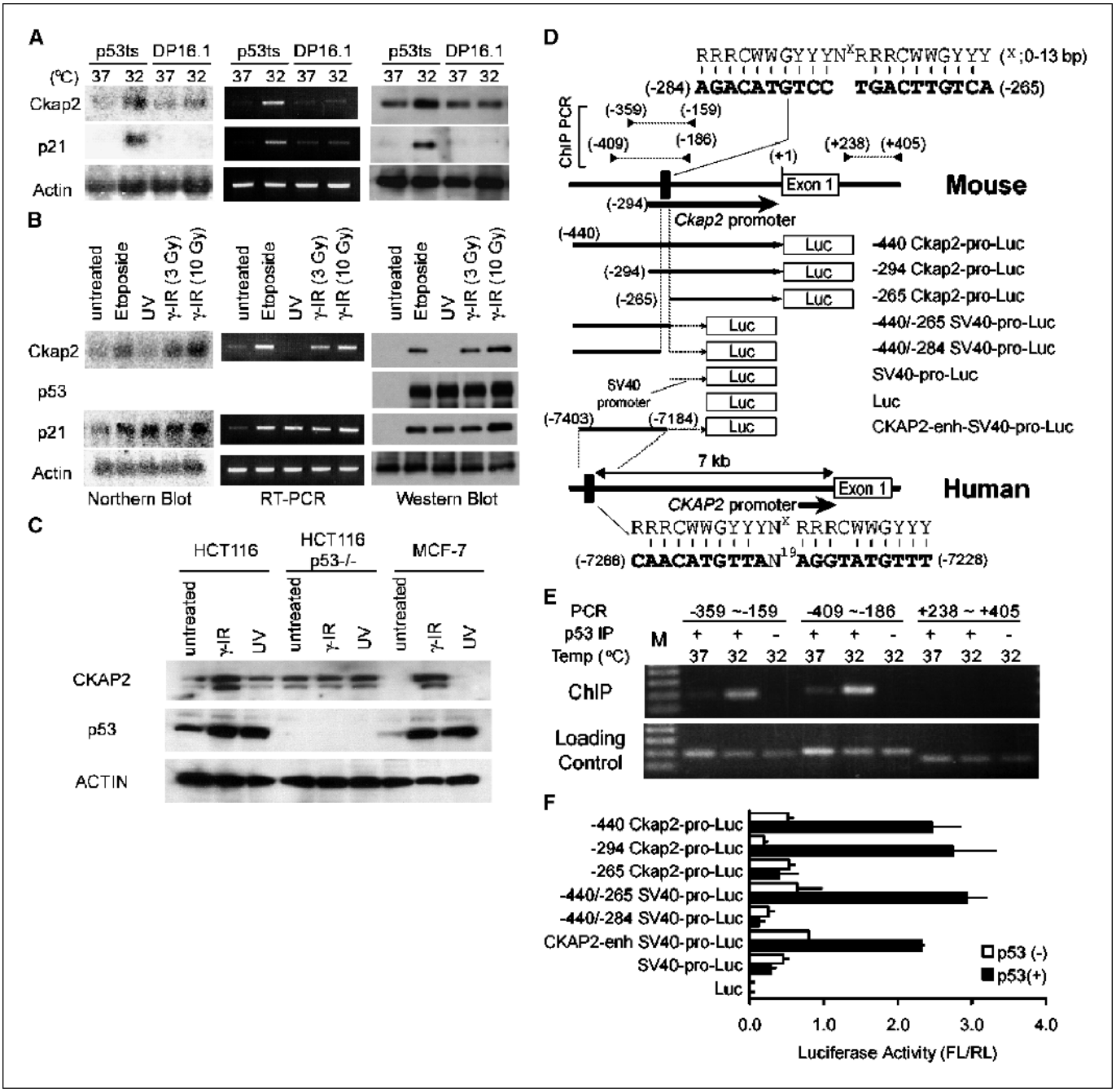

Figure 1. *Ckap2* is transactivated by p53. *A,* p53 dependence of *Ckap2* mRNA and protein induction in mouse erythroleukemia cells. DP16.1 (control) and DP16.1/p53ts (p53ts) cells were temperature-shifted to activate p53 in the latter. *Left,* Northern blot of total RNA (10 μg) prepared from cells grown for 6 hours at 37°C or 32°C. Probes were cDNAs specific for *Ckap2, p21*^{Waf1}, or *actin. Middle,* RT-PCR detection of *Ckap2, p21*^{Waf1}, or *actin* of total RNA (1 μg) prepared from the same samples of Northern blot. *Right,* Western blot of total protein extracted from DP16.1 and DP16.1/p53ts cells grown at 37°C or 32°C for 8 hours. Detection was with anti-Ckap2, anti-p21^{Waf1}, and antiactin antibodies. *B,* induction of endogenous Ckap2 by DNA damage. WT mouse embryonic stem cells were exposed to 50 μmol/L etoposide, 50 mJ/cm^2 UV irradiation, or 3 or 10 Gy γ-irradiation and incubated for 6 or 8 hours for total RNA or total protein preparations, respectively. Probes for Northern blotting (*left*), RT-PCR (*middle*), and antibodies for Western blotting (*right*) were as for (*A*) and anti-p53. *C,* p53 dependence of CKAP2 induction in human cells. Western blot of total protein extracted from HCT116, HCT116 p53$^{-/-}$, and MCF-7 cells treated with 10 Gy γ-irradiation or 50 mJ/cm^2 UV irradiation. Both splice variants of CKAP2 protein were detected by the cross-reacting anti-Ckap2 antibody. *D,* structure of the upstream regions of the mouse *Ckap2* (*top*) and human *CKAP2* (*bottom*) loci. A TATA-less promoter (*bold arrow*) appears 294 nucleotides upstream of *Ckap2* exon 1. The potential p53-binding site (*bold lettering*) is shown beneath the p53 consensus binding site. Arrowheads indicate the PCR primers used for ChIP analysis. DNA fragments (*thin solid arrows*) from the *Ckap2* upstream region with (−440 Ckap2-pro; −294 Ckap2-pro) or without (−265 Ckap2-pro) the p53-binding site were used to generate the luciferase (Luc) reporters −440 Ckap2-pro-Luc, −294 Ckap2-pro-Luc, or −265 Ckap2-pro-Luc, respectively. Similarly, fragments containing (−440/−265) or lacking (−440/−284) the p53-binding site were subcloned in front of the SV40 promoter (*thin dotted arrows*) followed by Luc. A DNA fragment (−7,403/−7,184) containing with putative p53-binding site of human *CKAP2* was subcloned in front of SV40-Luc to generate CKAP2-enh-SV40-pro-Luc. *E,* ChIP assay of p53 DNA-binding activity in DP16.1/p53ts cells. Cells were cultured at 32°C or 37°C for 6 hours. Cross-linked and fragmented p53-DNA complexes were immunoprecipitated with either anti-p53 antibody (p53 IP +) or normal rabbit serum (p53 IP −). Precipitated DNA was subjected to PCR using primers that amplified either promoter fragments containing the p53-binding site (−359 to −159 and −409 to −186), or the intron 1 region lacking the p53-binding site (+238 to +405). Unprecipitated genomic DNA was the loading control. *F,* luciferase activities of deletion mutants with or without the *Ckap2* or *CKAP2* p53-binding site following transfection into HCT116 p53$^{-/-}$ cells with (*open columns*) or without (*solid columns*) the p53 expression plasmid. Luc activities (*FL*) were normalized to the activity of simultaneously transfected pRL-TK (*RL*). *Columns,* mean FL/RL values (n = 3); *bars,* SE.

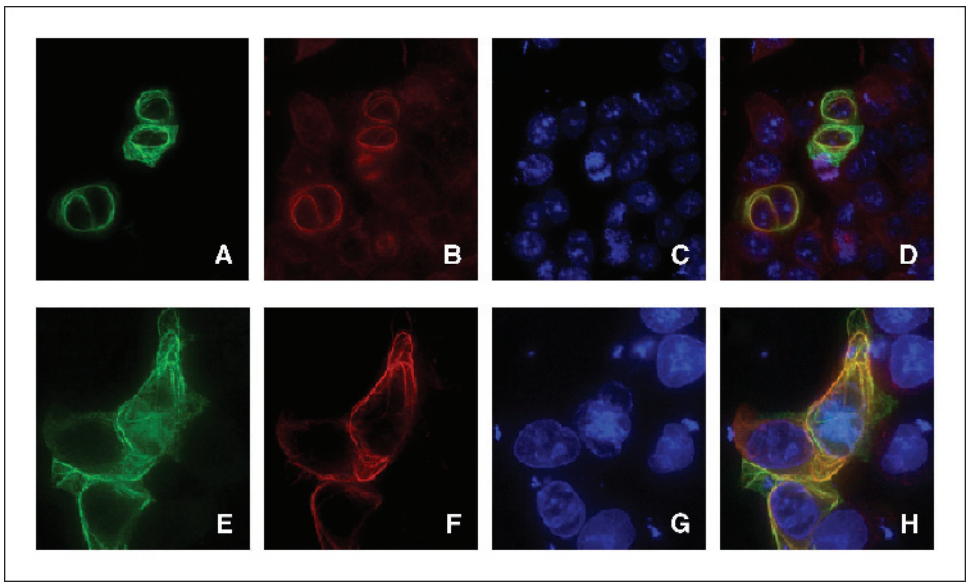

Figure 2. Overexpressed Ckap2 colocalizes with and stabilizes microtubules. HCT116 $p53^{-/-}$ cells were transfected with the EGFP-Ckap2 (1-648) expression plasmid, cultured for 48 hours, and fixed. Ckap2 expression was detected using an EGFP tag (*A* and *E, green*). Microtubules were visualized using anti–α-tubulin antibody (*B, red*), whereas stabilized microtubules were detected using anti–acetylated tubulin (*F, red*). Cell nuclei were stained with 4′,6-diamidino-2-phenylindole (DAPI; *C* and *G, blue*). Merged image shows the colocalization of overexpressed Ckap2 with microtubules (*D, yellow*). Microtubules were acetylated only in Ckap2-overexpressing cells (*H, yellow*).

promoter is derived from this region (Fig. 1*F*). Cotransfection of p53 increased the luciferase activity of constructs containing the putative p53-binding site (−440 Ckap2-pro-Luc, −294 Ckap2-pro-Luc) but not a construct lacking this site (−265 Ckap2-pro-Luc). Luciferase activity was also induced by chimeric promoters containing the SV40 promoter plus the *Ckap2* upstream region or the human *CKAP2* enhancer. p53 overexpression enhanced the activity of constructs containing the p53-binding site (−440/−265

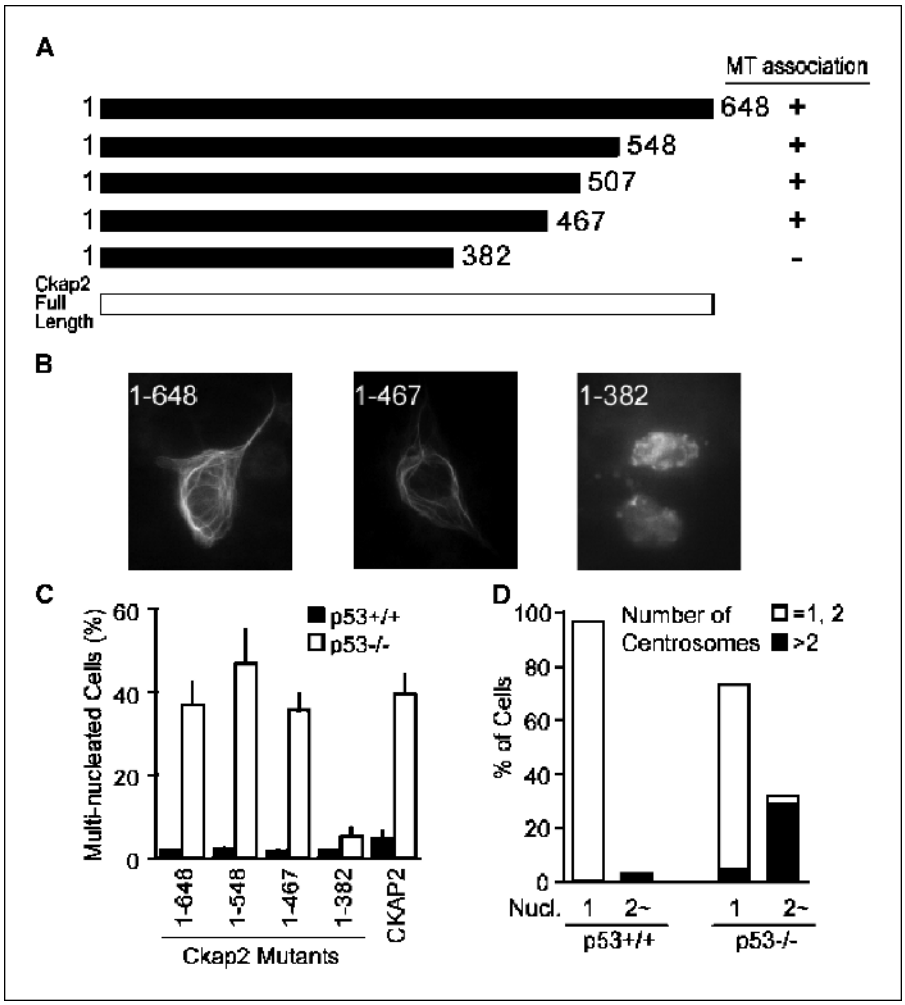

Figure 3. Microtubule-associated Ckap2 induces nuclear abnormalities. *A,* schematic representation of Ckap2 variants and their association with microtubules (*MT*). *B,* localization of Ckap2 deletion mutants. NIH3T3 cells were transfected with EGFP-Ckap2 (1-648), EGFP-Ckap2 (1-467), or EGFP-Ckap2 (1-382), and subcellular distribution was detected by fluorescence microscopy. *C,* microtubule-associated Ckap2 induces multinucleate cells. HCT116 ($p53^{+/+}$) or HCT116 $p53^{-/-}$ cells were transfected with the indicated EGFP-Ckap2 deletion mutants or CKAP2. After 48 hours, nuclei were fixed and stained with DAPI and GFP-positive cells showing multiple nuclei were counted. At least 300 cells were examined per transfection. *Columns,* mean percentage of multinucleate cells ($n = 3$); *bars,* SE. *D,* Ckap2 induces centrosome amplification. HCT116 ($p53^{+/+}$) or HCT116 $p53^{-/-}$ cells were transfected with EGFP-Ckap2 (1-648) and centrosomes were detected 48 hours later with anti–γ-tubulin antibody. Centrosomes in 100 GFP-positive cells were counted per culture. *Columns,* percentage of total GFP-positive cells that were mononuclear (Nucl = 1) or binuclear (Nucl = 2), and the percentage of each of these groups of cells that contained the indicated numbers of centrosomes. Results shown are the average of duplicate experiments.

SV40-pro-Luc and CKAP2-enh SV40-pro-Luc) but not that of the construct lacking the p53-binding site (−440/−284 SV40-pro-Luc).

Ckap2 stabilizes microtubules. Our recombinant mouse Ckap2 protein colocalized with the cytoskeleton (Fig. 2), consistent with previous reports (7–9). Transfected full-length EGFP-Ckap2 was distributed in a fine reticular pattern (Fig. 2*A*). Comparison of this pattern with patterns generated by α-tubulin immunostaining (Fig. 2*B*) or nuclear staining (Fig. 2*C*) suggested that Ckap2 associated with cytoplasmic microtubules. Indeed, the overlay image revealed colocalization of Ckap2 and α-tubulin (Fig. 2*D*). Closer examination of microtubules associated with Ckap2 showed a thick bundle-like pattern characteristic of hyperstabilization (Fig. 2*A, B*, and *D*). Antiacetylated tubulin antibody, which detects stabilized microtubules (Fig. 2*F*), bound to tubulin only in Ckap2-expressing cells (GFP-positive cells; Fig. 2*E* and *G*), whereas tubulin proteins in untransfected cells (GFP-negative cells; Fig. 2*E* and *G*) were not acetylated (Fig. 2*H*). This microtubule hyperstabilization was p53 independent, because HCT116 cells transfected with the EGFP-Ckap2 showed the same bundle-like microtubules and tubulin acetylation pattern (data not shown). The microtubular localization of Ckap2 was also reproducibly observed in mouse fibroblasts and HeLa cells (data not shown). The tagging of Ckap2 did not influence its localization because HCT116 $p53^{-/-}$ cells transfected with untagged mouse Ckap2 or human CKAP2 cDNA showed the same pattern of microtubular association and hyperstabilization upon staining with anti-Ckap2 antibody (data not shown).

Microtubule-associated Ckap2 induces the formation of multiple nuclei and abnormal centrosome numbers in a p53-dependent manner. The central region of the Ckap2 protein is required for microtubular association (7). We constructed a series of deletion mutants and transfected them into HCT116 and NIH3T3 cells. COOH-terminal deletion mutants lacking up to 202 amino acids (Ckap2 1-588, 1-548, 1-507, and 1-467) showed reticular cytoplasmic localization and thick bundle-like pattern as same as full-length (1-648) Ckap2 (Fig. 3*A* and *B*). However, the Ckap2 (1-382) mutant showed speckled nuclear localization rather than microtubule-associated cytoplasmic distribution (Fig. 3*B*).

Upon inspection of HCT116 $p53^{-/-}$ cells overexpressing microtubule-associated Ckap2 mutants or full-length human CKAP2, we found that 30% to 50% of these cells harbored double nuclei (Fig. 3*C* and Supplementary Fig. S1; also visible in Fig. 2*D* and *H*). Double nuclei were not present in Ckap2-expressing HCT116 cells (Fig. 3*C*). Significantly, the number of binuclear cells was reduced for the one mutant (Ckap2 1-382) that did not associate with microtubules. Thus, binuclear cells appear only when Ckap2 associates with microtubules in the absence of p53.

Costaining of γ-tubulin as a centrosome marker revealed that 90% of the binuclear cells in Ckap2-expressing HCT116 $p53^{-/-}$ cultures showed abnormal centrosome amplification, whereas mononuclear cells had normal centrosome numbers (Fig. 3*D*; Supplementary Fig. S1). These data imply that extra centrosomes might have arisen as a consequence of aborted cell divisions, which in turn gave rise to tetraploidy, rather than the result of the abnormal centrosome amplification during the S phase (17).

Ckap2 enhances p53 functions. Previous reports suggested that p53 is frequently activated by the treatments that induce polyploidy (4, 5). To evaluate the effect of Ckap2 on endogenous p53, EGFP-Ckap2 was transfected into HCT116 cells and endogenous p53 protein and mRNA in total cell lysates were detected by Western blotting and RT-PCR. HCT116 cells expressing full-length Ckap2 (1-648), but not truncated Ckap2 (1-382), showed higher levels of endogenous p53 protein compared with cells transfected with a GFP control vector whereas *p53* mRNA level was not changed (data not shown). Additional etoposide treatment of transfected cells enhances the effect of full-length Ckap2 protein-induced p53 protein level

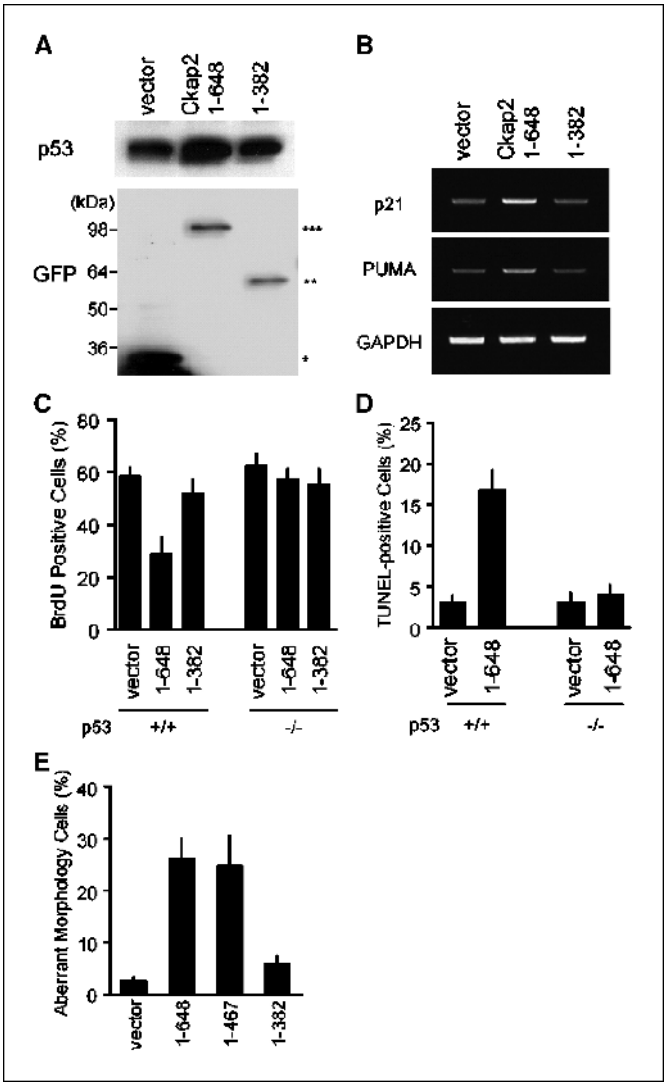

Figure 4. Overexpressed Ckap2 increases p53 protein levels and activities. *A,* increased endogenous p53 protein. HCT116 cells were transfected with EGFP-Ckap2 (1-648), EGFP-Ckap2 (1-382), or EGFP (vector). Cells were selected in puromycin for 48 hours and total protein was subjected to Western blotting using anti-p53 antibody. EGFP-Ckap2 1-648 (***), EGFP-Ckap2 (1-382) (**), and EGFP (*) proteins were detected at their expected sizes by anti-GFP antibody. *B,* increased expression of p53 target genes. HCT116 and HCT116 $p53^{-/-}$ cells were transfected with either empty vector, Ckap2 1-648, or Ckap2 1-382 as for (*A*). Transcripts of $p21^{WAF1}$, *PUMA*, and *GAPDH* were detected by RT-PCR. *C,* reduced S-phase population. HCT116 ($p53^{+/+}$) and HCT116 $p53^{-/-}$ ($p53^{-/-}$) cells were transfected with EGFP (vector) or the indicated EGFP-Ckap2 variants and S-phase cells were evaluated 48 hours later by BrdUrd incorporation. *Columns,* mean percentage of BrdUrd-positive cells ($n = 3$); *bars,* SE. *D,* induction of p53-dependent apoptosis. HCT116 ($p53^{+/+}$) and HCT116 $p53^{-/-}$ cells were transfected with control (vector) or Ckap2 (1-648) and fixed 48 hours later. Apoptotic cells in the Ckap2-overexpressing population were detected by terminal deoxynucleotidyl transferase–mediated nick end labeling (TUNEL) staining. *Columns,* mean percentage of Ckap2-expressing cells that were also TUNEL positive ($n = 3$); *bars,* SE. *E,* induction of cell death by microtubule-associated Ckap2. HCT116 cells were transfected with empty vector or the indicated EGFP-Ckap2 variants and aberrant morphology characteristic of cell death was evaluated 48 hours later. The Ckap2 (1-382) mutant does not associate with microtubules. *Columns,* mean percentage of GFP-positive cells that had aberrant morphology ($n = 3$); *bars,* SE.

(Fig. 4*A*). Furthermore, overexpression of full-length Ckap2 (but not truncated Ckap2) enhanced luciferase activity driven by either the p53 response element, the *p21*^{WAF1} promoter, or the *Bax* promoter (Supplementary Fig. S2). RT-PCR confirmed that Ckap2 overexpression in HCT116 cells enhanced the induction of the p53 target genes *p21* and *PUMA* (Fig. 4*B*).

To determine whether Ckap2 contributes to cell cycle regulation, the S-phase populations of Ckap2-transfected HCT116 and HCT116 p53$^{-/-}$ cells were evaluated by BrdUrd incorporation. Ckap2 transfection reduced the proportion of HCT116, but not HCT116 p53$^{-/-}$, cells that was in S phase (Fig. 4*C*), suggesting that Ckap2 arrests the cell cycle in p53-dependent manner. Transfection of HCT116 cells with Ckap2 (1-382) resulted in negligible S-phase reduction (Fig. 4*C*), indicating that Ckap2 must be associated with microtubules to reduce S-phase populations.

To assess whether Ckap2 contributes to cell death, apoptosis was evaluated in Ckap2-transfected HCT116 and HCT116 p53$^{-/-}$ cells by TUNEL staining. Ckap2 induced apoptosis only in HCT116 cells (Fig. 4*D*). Variants of Ckap2 that associated with microtubules (Ckap2 1-648 and 1-467) induced aberrant morphology characteristic of cellular toxicity (Fig. 4*E*; Supplementary Fig. S3), whereas transfection of Ckap2 1-382 or EGFP resulted in significantly fewer dead cells.

To investigate whether Ckap2 influences proliferation, we overexpressed full-length Ckap2 in HCT116 and HCT116 p53$^{-/-}$ cells, cultured the cells for 14 days, and counted colonies of diameter >1 mm. Ckap2 expression profoundly reduced colony formation in HCT116 cultures but had only a modest effect on HCT116 p53$^{-/-}$ colony formation (Supplementary Fig. S4).

Discussion

Recent evidence suggests that DNA-damaging agents activate a small subset of common target genes, but that p53 then induces a unique constellation of genes depending on the stimulus (2). *Ckap2*, which we identified as a novel p53 target gene whose product colocalizes with microtubules, may be such a stimulus-specific target gene. The mouse *Ckap2* promoter and the human *CKAP2* upstream region contain well-conserved p53-binding sites to which p53 protein binds directly, enhancing the expression of downstream genes. Significantly, p53-mediated Ckap2 up-regulation occurs in response to γ-irradiation and etoposide treatment but not UV irradiation.

Overexpression of Ckap2 induces hyperstabilization of microtubules (Fig. 2). Aberrant stabilization of tubulin polymers leads to disturbed spindle function, which in turn results in cytokinesis defects and ultimately tetraploidy (4). Although "p53-mediated tetraploid checkpoint" is still an issue of controversy, p53 is frequently activated in cells undergo cytokinesis failure and prevents further proliferation of these cells (17–19). Our study showed that microtubule-associated Ckap2 induces aberrant centrosome numbers and double nuclei formation in the absence of p53. In parallel, Ckap2 overexpression results in endogenous p53 activation, decreased S-phase cells, and increased apoptosis. To test our hypothesis under physiologic conditions, we are developing an antibody that better detects endogenous Ckap2 proteins. RNA interference studies are not an option because cells in which CKAP2 is reduced by RNA interference quickly undergo mitotic catastrophe even in the absence of DNA damage (data not shown).

CKAP2 is highly expressed in gastric cancers and lymphomas but not in normal tissues surrounding these tumors (8, 9, 20). It may seem paradoxical that a target gene of the tumor suppressor p53 would be overexpressed in tumor cells, but there are precedents. The tumor suppressors VHL and RASSF1A interact with tubulin and induce aberrant microtubule stabilization followed by genetic instability (21–23). In addition, the cytokinesis-regulating protein PRC1 was recently identified as a negatively regulated transcriptional target of p53. Activated p53 reduces PRC1 levels, followed by cytokinesis defects and tetraploidy (24). We picture a physiologic feedback loop in which up-regulation of Ckap2, VHL or RASSF1A, or down-regulation of PRC, initially induces tetraploidy. p53 and the tetraploidy checkpoint are subsequently activated such that the abnormal cells are eliminated before they can become aneuploid and promote tumorigenesis. However, the p53 pathway is likely already inactivated in most of tumor cells, eventually overexpressed CKAP2 induces aneuploidy leading to genomic instability and tumorigenesis rather than cell death. Our work suggests that the regulation of microtubule dynamics, as mediated by proteins such as Ckap2, may be vital for tumor suppression.

Acknowledgments

Received 11/24/2004; revised 3/22/2005; accepted 4/28/2005.

Grant support: Terry Fox Cancer Foundation and Canadian Institutes of Health Research grants (T.W. Mak), and a Canadian Institutes of Health Research fellowship (K. Tsuchihara).

The costs of publication of this article were defrayed in part by the payment of page charges. This article must therefore be hereby marked *advertisement* in accordance with 18 U.S.C. Section 1734 solely to indicate this fact.

We thank Ikuko Hayashi for helpful advice and discussions, Denis Bouchard and Julie Vezina for technical assistance, and Mary Saunders for scientific editing.

References

1. Vousden KH, Lu X. Live or let die: the cell's response to p53. Nat Rev Cancer 2002;2:594–604.
2. Zhao R, Gish K, Murphy M, et al. Analysis of p53-regulated gene expression patterns using oligonucleotide arrays. Genes Dev 2000;14:981–93.
3. Wang L, Wu Q, Qiu P, et al. Analyses of p53 target genes in the human genome by bioinformatic and microarray approaches. J Biol Chem 2001;276:43604–10.
4. Andreassen PR, Lohez OD, Margolis RL. G_2 and spindle assembly checkpoint adaptation, and tetraploidy arrest: implications for intrinsic and chemically induced genomic instability. Mutat Res 2003;532:245–53.
5. Stukenberg PT. Triggering p53 after cytokinesis failure. J Cell Biol 2004;165:607–8.
6. Uetake Y, Sluder G. Cell cycle progression after cleavage failure: mammalian somatic cells do not possess a "tetraploidy checkpoint". J Cell Biol 2004;165:609–15.
7. Jin Y, Murakumo Y, Ueno K, et al. Identification of a mouse cytoskeleton-associated protein, CKAP2, with microtubule-stabilizing properties. Cancer Sci 2004;95:815–21.
8. Maouche-Chretien L, Deleu N, Badoual C, et al. Identification of a novel cDNA, encoding a cytoskeletal associated protein, differentially expressed in diffuse large B cell lymphomas. Oncogene 1998;17:1245–51.
9. Bae CD, Sung YS, Jeon SM, et al. Up-regulation of cytoskeletal-associated protein 2 in primary human gastric adenocarcinomas. J Cancer Res Clin Oncol 2003;129:621–30.
10. Prestridge DS. Predicting Pol II promoter sequences using transcription factor binding sites. J Mol Biol 1995;249:923–32.
11. Tsunoda T, Takagi T. Estimating transcription factor bindability on DNA. Bioinformatics 1999;15:622–30.
12. Okada H, Bakal C, Shahinian A, et al. Survivin loss in thymocytes triggers p53-mediated growth arrest and p53-independent cell death. J Exp Med 2004;199:399–410.
13. Morgenstern JP, Land H. Advanced mammalian gene transfer: high titre retroviral vectors with multiple

drug selection markers and a complementary helper-free packaging cell line. Nucleic Acids Res 1990;18:3587–96.
14. Wen SF, Xie L, McDonald M, et al. Development and validation of sensitive assays to quantitate gene expression after p53 gene therapy and paclitaxel chemotherapy using *in vivo* dosing in tumor xenograft models. Cancer Gene Ther 2000;7:1469–80.
15. Johnson P, Chung S, Benchimol S. Growth suppression of Friend virus-transformed erythroleukemia cells by p53 protein is accompanied by hemoglobin production and is sensitive to erythropoietin. Mol Cell Biol 1993;13:1456–63.
16. El-Deiry WS, Kern SE, Pietenpol JA, et al. Definition of a consensus binding site for p53. Nat Genet 1992;1:45–9.
17. Meraldi P, Honda R, Nigg EA. Aurora-A overexpression reveals tetraploidization as a major route to centrosome amplification in $p53^{-/-}$ cells. EMBO J 2002;21:483–92.
18. Borel F, Lohez OD, Lacroix FB, et al. Multiple centrosomes arise from tetraploidy checkpoint failure and mitotic centrosome clusters in p53 and RB pocket protein-compromised cells. Proc Natl Acad Sci U S A 2002;99:9819–24.
19. Yamaguchi H, Chen J, Bhalla K, Wang HG. Regulation of Bax activation and apoptotic response to microtubule-damaging agents by p53 transcription-dependent and -independent pathways. J Biol Chem 2004;279:39431–7.
20. Eichmuller S, Usener D, Dummer R, et al. Serological detection of cutaneous T-cell lymphoma-associated antigens. Proc Natl Acad Sci U S A 2001;98:629–34.
21. Hergovich A, Lisztwan J, Barry R, Ballschmieter P, Krek W. Regulation of microtubule stability by the von Hippel-Lindau tumour suppressor protein pVHL. Nat Cell Biol 2003;5:64–70.
22. Dallol A, Agathanggelou A, Fenton SL, et al. RASSF1A interacts with microtubule-associated proteins and modulates microtubule dynamics. Cancer Res 2004;64:4112–6.
23. Vos MD, Martinez A, Elam C, et al. A role for the RASSF1A tumor suppressor in the regulation of tubulin polymerization and genomic stability. Cancer Res 2004;64:4244–50.
24. Li C, Lin M, Liu J. Identification of *PRC1* as the p53 target gene uncovers a novel function of p53 in the regulation of cytokinesis. Oncogene 2004;23:9336–47.

Ckap2 Regulates Aneuploidy, Cell Cycling, and Cell Death in a p53-Dependent Manner

Katsuya Tsuchihara, Valentina Lapin, Christopher Bakal, et al.

Cancer Res 2005;65:6685-6691.